

## Article

# Bio-Assisted Leaching of Non-Ferrous Metals from Waste Printed Circuit Boards—Importance of Process Parameters

Arevik Vardanyan <sup>1,2</sup>, Narine Vardanyan <sup>1</sup>, Mohamed Aâtach <sup>2</sup>, Pierre Malavasi <sup>2</sup> and Stoyan Gaydardzhiev <sup>2,\*</sup>

<sup>1</sup> Department of Microbiology, SPC “Armbiotechnology” of the National Academy of Sciences of Armenia, 14 Gyurjyan Str., Yerevan 0056, Armenia

<sup>2</sup> GeMMe—Minerals Engineering and Recycling, Faculty of Applied Sciences, ArGenCo Department, University of Liege, Allée de la découverte 9, Bât. B52/3, Sart-Tilman, 4000 Liege, Belgium

\* Correspondence: s.gaydardzhiev@uliege.be; Tel.: +32-(43)-669120

**Abstract:** The effect of varying process parameters during bio-catalyzed leaching of metals from end-of-life printed circuit boards (PCBs) was investigated. Fragmented PCBs (under 2 mm) were subjected to an indirect bioleaching in a stirred tank reactor while pulp density, pH and initial ferric iron content were varied. An iron oxidizing *Acidithiobacillus ferrooxidans* 61 microbial strain was used to generate the lixiviant through oxidizing Fe(II) to Fe(III). Chemically generated Fe(III) was tested as lixiviant under the same conditions as the biological one for comparative purposes. Cell enumeration during leaching and microscopic observations of the input and leached PCBs were conducted in parallel to shed light on the observed phenomena. The degree of bringing metals in solution was found to depend mainly on ferric iron concentration and pH. For the entire duration being always kept as 24 h, substantial portion of Cu (~87%) was extracted respectively at 1% pulp density (PD), 15.5 g/L Fe<sup>3+</sup> and pH 1. For Zn and Ni, nearly 100% recovery was observed at 5% PD, 18 g/L Fe<sup>3+</sup> and pH 1.1. The achieved results offer possibilities for further studies at higher pulp density, to ultimately render the bioleaching approach as enabling economical and environmentally friendly technology for urban mining of non-ferrous metals.



**Citation:** Vardanyan, A.; Vardanyan, N.; Aâtach, M.; Malavasi, P.; Gaydardzhiev, S. Bio-Assisted Leaching of Non-Ferrous Metals from Waste Printed Circuit Boards—Importance of Process Parameters. *Metals* **2022**, *12*, 2092. <https://doi.org/10.3390/met12122092>

Academic Editor: Stefano Ubaldini

Received: 30 October 2022

Accepted: 2 December 2022

Published: 6 December 2022

**Publisher’s Note:** MDPI stays neutral with regard to jurisdictional claims in published maps and institutional affiliations.



**Copyright:** © 2022 by the authors. Licensee MDPI, Basel, Switzerland. This article is an open access article distributed under the terms and conditions of the Creative Commons Attribution (CC BY) license (<https://creativecommons.org/licenses/by/4.0/>).

**Keywords:** printed circuit boards (PCB); iron oxidizing bacteria; double-stage bioleaching; metal extraction; pulp density; leaching yield

## 1. Introduction

Advanced electronic equipment is in high demand due to ongoing technological development, and as a consequence is characterized by relatively short lifespan [1]. This situation reflects in an unparallel accumulation of end-of-life electronic devices, commonly classified as electronic waste. According to the United Nations, the global generation of electronic waste (e-waste) streams was estimated between 20 and 50 million tons per year [2]. The main problem with e-waste is its toxicity, which is caused by the presence of hazardous metals (Ni, Cd, Se, As, Cr and Pb), brominated flame retardants, polychlorinated biphenyls and epoxy-based materials [3–5].

Printed circuit boards (PCBs), on the other hand, could turn an important source of base and precious metals, providing an economic incentive for recycling [6–11]. PCBs typically have a content of 30–40% metals, 30% plastics and 30% glass and oxides [12–17]. Thus, it is clear that there is a critical need for e-waste recycling and material valorization, which strengthen the supply chain’s sustainability and support the circular economy. Several pyro- and hydrometallurgical studies have been carried out to recover metals from PCBs [2,18–21]. The application of pyrometallurgy for base metals recovery implies carrying out processes at higher temperatures, which provokes environmental concerns linked to gas emissions and slag generation [22]. On the other hand, conventional hydrometallurgical processes rely on intensive use of acids and supporting chemicals.

Organic acids, which are less corrosive and more selective than inorganic ones, can also be used for metal extraction [23]. Through acidification and complexation mechanisms they can solubilize the metallic fractions of oxidized or zero-valent metal bearing compounds [24]. Metals can also be recovered from e-waste through bio-hydrometallurgical routes, which are well-established in non-ferrous metal mining, and in some operations have proven more efficient than classical hydrometallurgical processes due to lower environmental footprint and demonstrated cost competitiveness [25,26].

Biohydrometallurgy encompasses main metallurgical steps such as leaching, solution purification and recovery of valuable metals. Bioleaching, one of the most-studied unit operations in biohydrometallurgy, enables non-negligible reduction in reagent use because they are produced in situ by microorganisms under soft operating conditions, i.e., low temperatures and mild pH [27]. On the other hand, biohydrometallurgy is less polluting and offers reduced operating costs and energy demand [28].

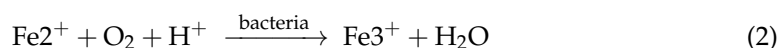
Various chemolithotrophic microorganisms are used in bioleaching applications thanks to their ability to facilitate metal dissolution via series of bio-oxidation reactions [29–34]. Iron exercise a central role as an electron carrier inside the bioleaching system. The oxidized form of iron (Fe(III)), which is generated by the microbial oxidation of ferrous iron (Fe(II)) substrates, acts as an oxidizing agent capable of oxidizing metal sulfides before being chemically reduced to ferrous iron [35].

Acid leaching is supported by acidophilic autotrophs, such as *Acidithiobacillus thiooxidans* [36], producing sulfuric acid in the presence of thiosulphate/sulfur/sulfide, while oxidation is performed by ferric iron produced by acidophilic iron-oxidizing autotrophs, such as *Acidithiobacillus ferrooxidans* [3,37] and *Leptospirillum ferrooxidans* [3].

Several studies have been conducted using microorganisms to extract metals from PCBs [18,31,37,38]. Recently, various chelating agents have been used in conjunction with microorganisms to improve metal extraction. Pyrite is used as an alternative source of iron in mineral processing industries, acting as an energy source for the growth of iron oxidizers. However, the majority of the studies deals with very low pulp densities and report low metal extraction efficiency and slow metal extraction rates [19,23,37,39,40].

Acidophilic heterotrophic bacteria and fungi are also used for metal leaching processes with *Acinetobacter* [41], *Acidiphilium* [42], *Aspergillus niger* [43,44], *Aspergillus fumigatus* [45], *Pseudomonas aeruginosa* [46], *Chromobacterium violaceum* [46–48] being primarily used for bioleaching, either as a pure culture or as part of a consortium.

Brandl et al., 2001 [31] presumably was the first study on published PCB bioleaching, which relied on acidophilic microorganisms. The two main reactions that occur are:



Metals are oxidized by Fe(III), which is reduced into Fe(II)—Equation (1). The bacteria then regenerate Fe(III) in the presence of dissolved oxygen, according to Equation (2). In the absence of bacteria, the oxidation of Fe(II) is slow, but the presence of iron oxidizing bacteria in the system significantly accelerates Fe(III) regeneration. Fe(III) is known as a low-cost oxidation agent frequently used in hydrometallurgy and is particularly suited to leaching various metals from PCBs [49].

Several published studies have focused on the feasibility of PCB bioleaching in batch mode using shake flasks and bioreactors [50–53]. However, due to their notorious heterogeneity their bioleaching should ideally be investigated using large volume stirred tank reactors (>1 L), enabling a sufficient amount of material to be processed. Such conditions guarantee efficient reactant transport and mimic the industrial situation closely [17]. Studies also show that staggered addition of PCBs with continuous biological production of an acidic lixiviant containing Fe(III) do improve bioleaching efficiency, most likely due to reduced PCB toxicity on microbial growth [17,31,40].

The toxicity of metals on microbial growth can be addressed using an indirect leaching approach in which lixiviant production and e-waste leaching are separated into two-stage processes. This concept has been demonstrated successfully in a laboratory for leaching metals from lithium-ion batteries [54] and PCBs [17,55].

On the background of the above, the presented study aimed at investigating recovery of copper, zinc, nickel and aluminum from PCBs using culture-bearing solutions obtained from an acidophilic iron-oxidizing bacteria, namely *Acidithiobacillus ferrooxidans* 61. An indirect bioleaching approach performed as either single or double-stage mode was chosen to counterbalance the potential toxicity of the PCBs on microbial growth and activity. By decoupling biolixiviant generation and bioleaching steps, an increased efficiency of metal leaching was expected.

## 2. Materials and Methods

### 2.1. PCBs

Depopulated end-of-life PCBs were fragmented down to a particle size below 22 mm by a hammer mill (Laarmann CHM4000) run at 1750 rpm. The analysis of the input PCBs revealed the following concentrations of non-ferrous metals: Cu (21.2%), Zn (1%), Ni (0.1%), Al (2.2%). Ahead of the bioleaching, the surface passivation layer (green lacquer mask) was removed by boiling the fragmented PCBs in a 10% NaOH solution for 15 min at ambient temperature. Afterwards, the samples were thoroughly washed with deionized water until neutral pH, dried at ambient temperature and preserved for leaching.

The main metal content in the prepared PCBs is shown in Table 1.

**Table 1.** Main metals concentration in the input PCBs.

Metal, %	Concentration
Cu	21.53
Al	6.95
Pb	3.2
Zn	0.78
Ni	5.12
Fe	3.86
Sn	1.98
Ag	0.097

### 2.2. Microorganisms and Culturing Conditions

The biolixiviant used for leaching was obtained on the basis of an iron-oxidizing culture of *Acidithiobacillus ferrooxidans* 61 isolated from Tandzut ore (Armenia) acid drainage water. Modified 9 K medium (0.5 g/L  $(\text{NH}_4)_2\text{SO}_4$ , 0.5 g/L  $\text{MgSO}_4 \times 7\text{H}_2\text{O}$ , 0.5 g/L  $\text{K}_2\text{HPO}_4$ , 0.05 g/L KCl, 0.01 g/L  $\text{Ca}(\text{NO}_3)_2$ ) with  $\text{FeSO}_4 \times 7\text{H}_2\text{O}$  having concentration between 44.2 and 124 g/L, depending on the target  $\text{Fe}^{3+}$  content, was used for cultivation and bioleaching experiments. 10N  $\text{H}_2\text{SO}_4$  solution was used to adjust pH.

### 2.3. Bioleaching of PCBs

For generating lixiviant for the indirect bioleaching, culture of *A. ferrooxidans* 61 was cultured in the absence of PCBs using a modified 9 K medium maintained under optimum growing conditions. The growth of bacteria was carried out inside a bio-fermenter (Bionet Baby 0) coupled to control unit, to follow gas supply, stirring rate, pH, Eh and temperature, illustrated in Figure 1a. The fermenter filled in with 2 L culture medium was inoculated at 10% ( $v/v$ ) and pH adjusted to 1.8–1.9. The fermenter was operated at temperature of 30 °C, stirring speed of 80 rpm and at 1 lpm air-flow. After 5–10 days of cultivation (depending on the concentration of ferrous sulfate), a reddish coloration of the culture medium was

observed due to oxidation of  $\text{Fe}^{2+}$  to  $\text{Fe}^{3+}$ , with concomitant bacterial growth reaching density of  $2.5 \times 10^6$ – $0.25 \times 10^9$  cells/mL and redox potential arriving in the range of 700 mV Ag/AgCl.

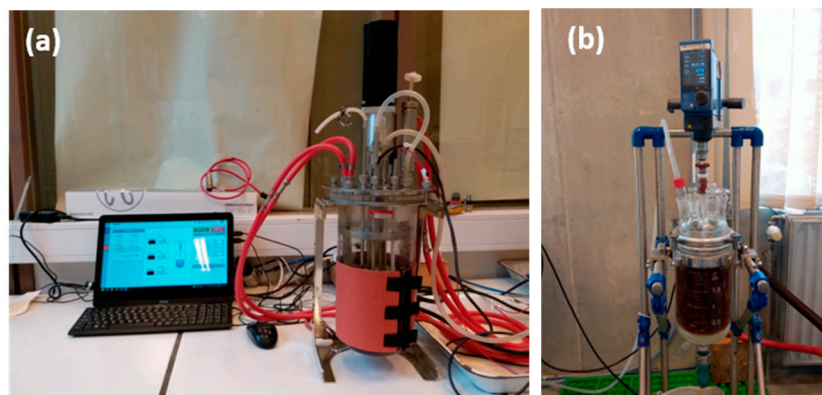


**Figure 1.** View of bio-fermenter (a) and stirred tank leaching reactor (b).

Indirect bioleaching of the PCBs was performed inside a 2 L jacketed reactor coupled to a circulating bath to maintain constant operating temperature of  $40^\circ$  needed to sustain eventual bacterial growth. The reactor was connected to a condenser to prevent excessive evaporation and a tunable compressor to supply air—Figure 1b.

Leaching tests were run for 24 h at  $40^\circ\text{C}$ , stirring rate of 600 rpm and an air supply of 1 lpm. Experiments were performed under pH 1, 1.1, 1.8 and 2.1, using the following concentrations of  $\text{Fe}^3$  as oxidizing agent (g/L): 9; 13.5, 15.5, 20 and 25. Pulp densities (PD) were varied at 1%, 3%, 5% and 10%. Sampling was performed at start-up, 1 h, 3 h, 5 h and 24 h. Quantitative determination of bacterial cells during the leaching was carried out by a serial end-point dilution methodology (e.g., “Most Probable Number” technique) [56]. The solid residues were air dried and subjected to chemical and mineralogical (XRD) analysis. To mimic industrial conditions to a maximum extent, all experiments were conducted without sterilization.

To outline the effect from the origin of  $\text{Fe}^{3+}$  used in the leaching, parallel to the biogenic ferric iron obtained from *A. ferrooxidans* 61, comparative trials using ferric iron of chemical origin ( $\text{Fe}_2(\text{SO}_4)_3$ ) were performed. The comparative tests were realized as two different modes—as single- and double-stage batches. When double-stage leaching was tested, the first stage had 2 h duration, after elapsing of which PLS was decanted and fresh lixiviant added directly to the remaining solid. This marked the beginning of a second-stage run for further 4 h.

#### 2.4. Analysis

Metals in the pregnant leach solution (PLS) were analyzed by atomic absorption spectrophotometry (AAS) and ICP-OES. The solid residue after leaching was dried, oven-treated at  $900^\circ\text{C}$  for 240 min, grinded in an agate mortar or a ring mill and digested in aqua regia before being analyzed, similar to the liquid samples. Ferrous and ferric iron concentration was determined by an EDTA-based complexometric titration [57].

Mineralogical inspection of the leached PCBs was realized on a Bruker (Billerica, MA, USA) D8 ECO diffractometer using  $\text{CuK}\alpha$  radiation ( $\text{Lambda} = 1.5418 \text{ \AA}$ ). Representative amount of the material was pulverized in an agate mortar, and then deposited on a zero background silicon sample-holder. The X-ray powder diffraction patterns were first interpreted using the EVA 3.2 software (Bruker, 2014). This software allowed us to identify the phases and compare them to the ICDD database, version PDF-2. Then, the powder patterns were analyzed using the TOPAS 4.2 software (Bruker, 2014), which allowed quantification of the mineral phases. The quantification procedure is based on the Rietveld method.

PCBs were observed on morphology and phases liberation by a SEM-based automated mineralogy system—Zeiss sigma 300 FEG “Mineralogic”—coupled to two Bruker EDS

xFlash 6|30 X-ray energy dispersion spectrometers (silicon drift detector). To this end, raw PCBs and samples derived after leaching were cast into 30 mm diameter resin mounts following an established procedure by [58]. The section polishing was accomplished by using polishing disks and diamond suspensions of different finesses. The SEM-EDS analyses were carried out using a probe current of 2.3 nA with an accelerating voltage of 20 kV at a working distance of 8.5 mm. A mapping mode was performed using a 3 to 5  $\mu\text{m}$  step size and a dwell time of 55 ms. Analytical conditions such as contrast and brightness were set up manually to provide best possible contrast between the observed phases (plastics, composites, metals). System magnification was set to 6000X and voltage tension to 20 kV.

Leaching kinetics (g L/h) was calculated using Equation (3) below:

$$\frac{d[\text{Cu}^{2+}]}{dt} = -\frac{d[\text{Fe}^{3+}]}{2 dt} \quad (3)$$

where:  $[\text{Cu}^{2+}]$ —variation in Cu concentration during the first and second hours;  
 $dt$ —leaching duration (hour).

Metal recovery was calculated following Equation (4) shown below:

$$\text{MR (\%)} = \frac{\text{CMI} \times V}{m \times \text{CMs}} \times 100 \quad (4)$$

where MR metal recovery, %;

CMI—concentration of leached metal in the pregnant leaching solution, %;

CMs—metal concentration in the feed, %;

m—mass of used PCBs, g;

V—volume of the leachate inside the reactor, mL (in our case 2000 mL).

### 3. Results and Discussion

#### 3.1. Effect of Initial Concentration of Fe(III), Pulp Density and pH on Metals Recovery

The effect of various concentrations of oxidizing agent (Fe(III)) at 1% PD and initial pH 1 on the recovery of Cu, Zn, Al and Ni is shown in Figure 2.

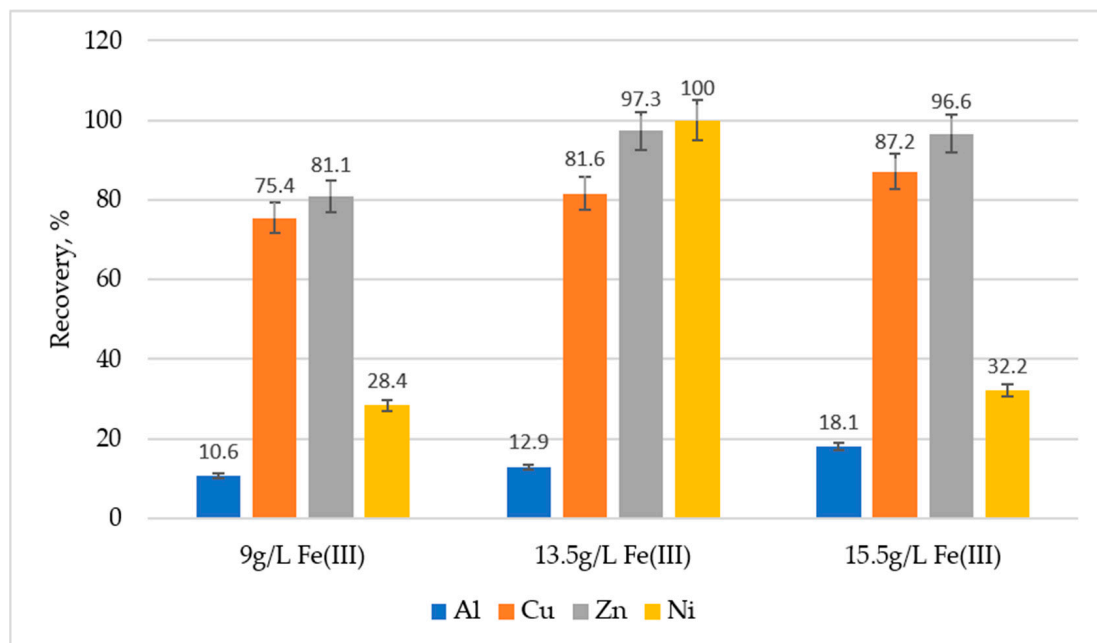


**Figure 2.** Recovery of metals from PCBs at various concentrations of biogenic  $\text{Fe}^{3+}$  (PD 1%; initial pH 1–1.1; 40 °C; air 1 lpm; 600 rpm; duration 24 h).

As shown in Figure 2, the ferric iron concentration exercises marked effect on copper recovery. During bioleaching at 40 °C, the increase of initial ferric iron concentration from 9 g/L to 15.5 g/L led to an increase in copper leaching rate from 0.6 g/L h to 1.5 g/L h, respectively. Thus, in the presence of 15.5 g/L Fe<sup>3+</sup> the maximum amount of recovered Cu within 24 h duration was about 87.2% at initial pH 1 and pulp density (PD) of 1%.

At pH 2.1 the recovery of Cu was 81.0% in the presence of 13.5 g/L Fe<sup>3+</sup>, which was roughly the same as at pH 1—81.6%, the rest conditions remained the same—Figure 3.

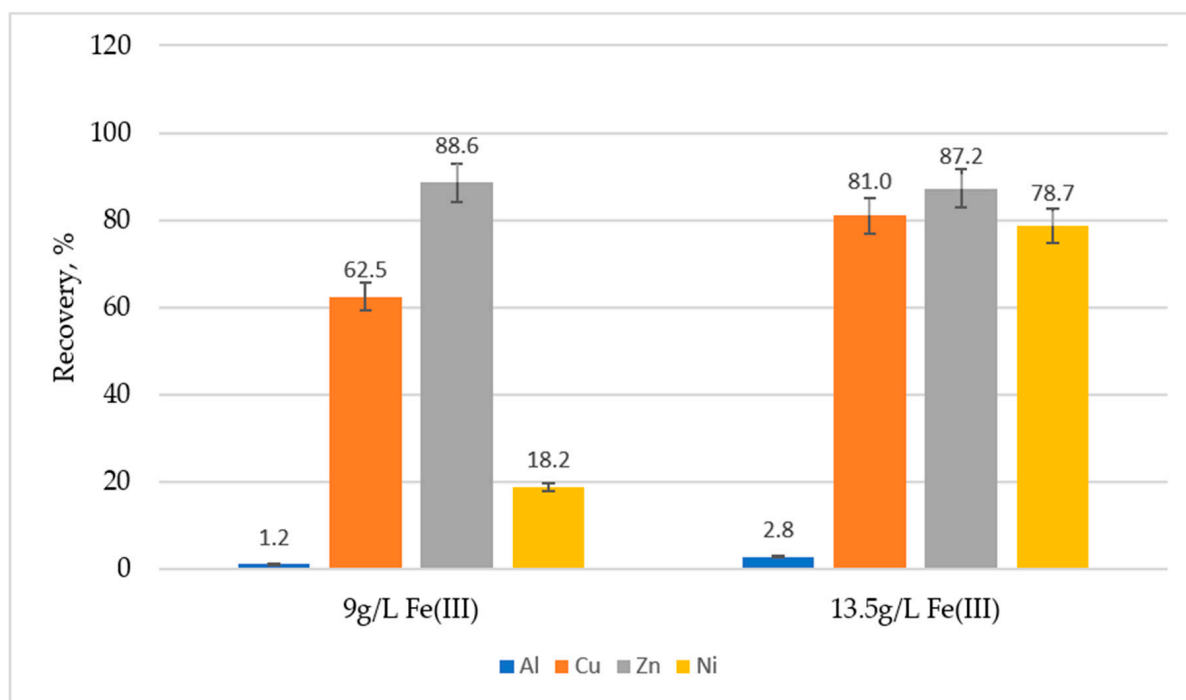


**Figure 3.** Recovery of metals from PCBs at 9 g/L and 13.5 g/L of biogenic Fe<sup>3+</sup> (PD 1%; initial pH 2.1; 40 °C; air 1 lpm; 600 rpm; duration 24 h).

It could be inferred that the recovery of Al at 1% PD is mostly related to the low pH and Fe<sup>3+</sup> concentration—Figure 2. The higher the amount of Fe<sup>3+</sup>, the higher the recovery of Al. The recovery of Al at pH 1.0 in the presence of 9 g/L and 13.5 g/L Fe<sup>3+</sup> was about 10.6% and 12.9%, respectively (Figure 2), while at higher pH (pH ≥ 2) it was about 9 and 4.6 times lower (1.2 and 2.8% respectively—Figure 3).

The recovery of Zn at 1% PD and pH 1 in the presence of 9 g/L, 13.5 g/L and 15.5 g/L Fe<sup>3+</sup> was about 81.1%, 97.3% and 96.6%, respectively (Figure 2). The recovery of Zn at pH 2 in the presence of 9 g/L was slightly higher to the one at pH 1, but lower at increased ferric iron (13.5 g/L) rate—88.6% and 87.2%, respectively. Therefore, in the case of Zn, it can be inferred that the initial concentration of Fe<sup>3+</sup> ions plays a secondary role and the initial pH is important.

As regarding Ni, its recovery in the presence of 9 g/L and 13.5 g/L Fe<sup>3+</sup> was about 28.4% and nearly 100% (Figure 2) at pH 1, and 18.2% and 78.7% at pH 2.1 (Figure 3). Thus, under acidic conditions an increase in Ni leachability was observed with an increase in the concentration of Fe<sup>3+</sup>.

It should be noted that if we consider the leaching duration, the metal recoveries reported in this paper are similar to those communicated by Hubau et al., 2020 [17]. Hubau et al. used a double-stage continuous bioleaching of PCBs shredded to 750 μm (without pretreatment) at 1% PD, pH 1.5, 40 °C and biolixiviant containing 8 g/L Fe<sup>3+</sup> obtained by bacterial acidophilic consortium BRGM-KCC comprising *Leptospirillum*, *Acidithiobacillus* and *Sulfobacillus* species. These conditions allowed them to recover 96% Cu, 85% Zn, 73% Ni and 54% Al over 48 h. On the other hand, Tapia et al., 2022 [28] managed to

recover 58.9% Zn and 65% Cu for 3 days and 91.3% Zn and 68.5% Cu for 15 and 11 days, respectively, from PCBs shredded to  $\leq 300\mu\text{m}$  (without pretreatment) at 1% of PD and 30 °C using bioleachant containing 9 g/L  $\text{Fe}^{3+}$  obtained by enriched acidophilic iron oxidizing consortium comprising seven cultures.

The follow-up of metals and  $\text{Fe}^{3+}$  content in the PLS with time is shown in Figure 4. As seen Al, Cu, Ni and Zn are brought in solution predominately during the first 5 h, a period followed by a plateau trend. In parallel, it can be seen that with  $\text{Fe}^{3+}$  consumption progressing metal extraction rate tended to slow down. This observation was probably caused either by a limited availability of  $\text{Fe}^{3+}$  because of generation of chemical complexes or due to a non-complete metal liberation from the PCB matrix.

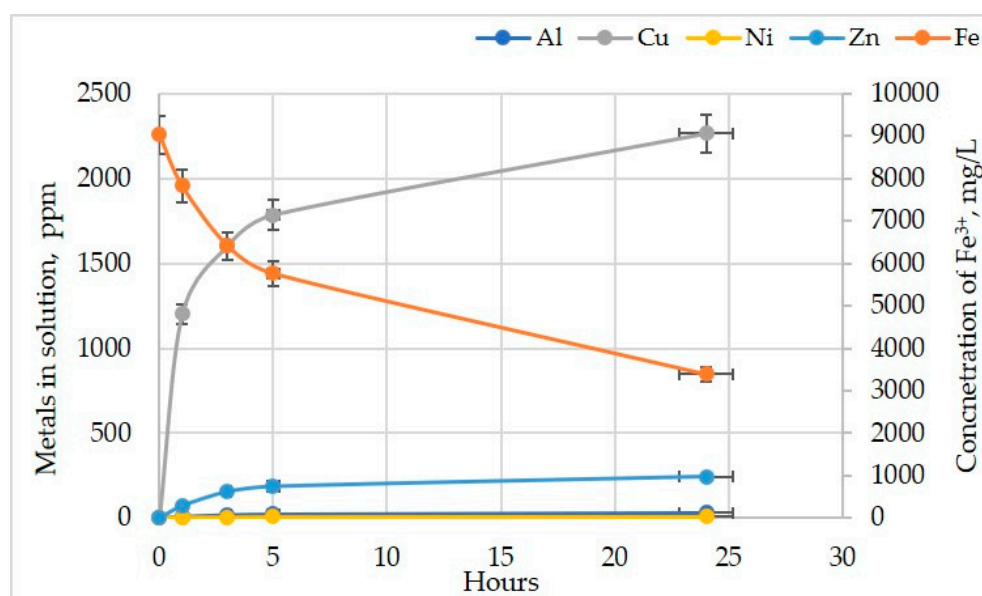


**Figure 4.** Evolution of metal ions and  $\text{Fe}^{3+}$  in the PLS with time (40 °C; 1% PD; pH 1.0; initial concentration of  $\text{Fe}^{3+}$  9/L).

When we compare the effect from the  $\text{Fe}^{3+}$  origin on the single-stage leaching efficiency at 5% PD, one might note that the recoveries of Cu at pH 2 in the presence of 20 g/L biogenic  $\text{Fe}^{3+}$  and 20 g/L chemical  $\text{Fe}^{3+}$  at pH 1.1 were virtually identical (67.5% and 65.8%, respectively)—Figure 5. A very similar pattern was observed for Zn and Ni. In case of Al, the recovery was very low in all four cases regardless initial pH and type of  $\text{Fe}^{3+}$  used. As mentioned elsewhere, maintaining highly acidic conditions in leaching is essential to promoting Al dissolution [59]. However, in our case, even at very low pH, Al was virtually not dissolved, probably due to intrinsic refractoriness (e.g., present as an alloy), surface coatings or encapsulation inside the PCB matrix.

The results from the comparative two-stage leaching using bio-derived  $\text{Fe}^{3+}$  (at 19 g/L) and chemically derived  $\text{Fe}^{3+}$  (at 16 g/L) are presented in Figure 6. In this series of tests PD was increased to 10%.

Perusal of the results shown in Figure 6 suggested that the recovery of Cu is virtually the same (62 and 61.5% for Cu) in chemical and biological leaching systems. Aluminum is brought into solution to a very modest extent (3–4%). Recovery of both Zn and Ni in the biological leaching system was about 20% higher than in the chemical.

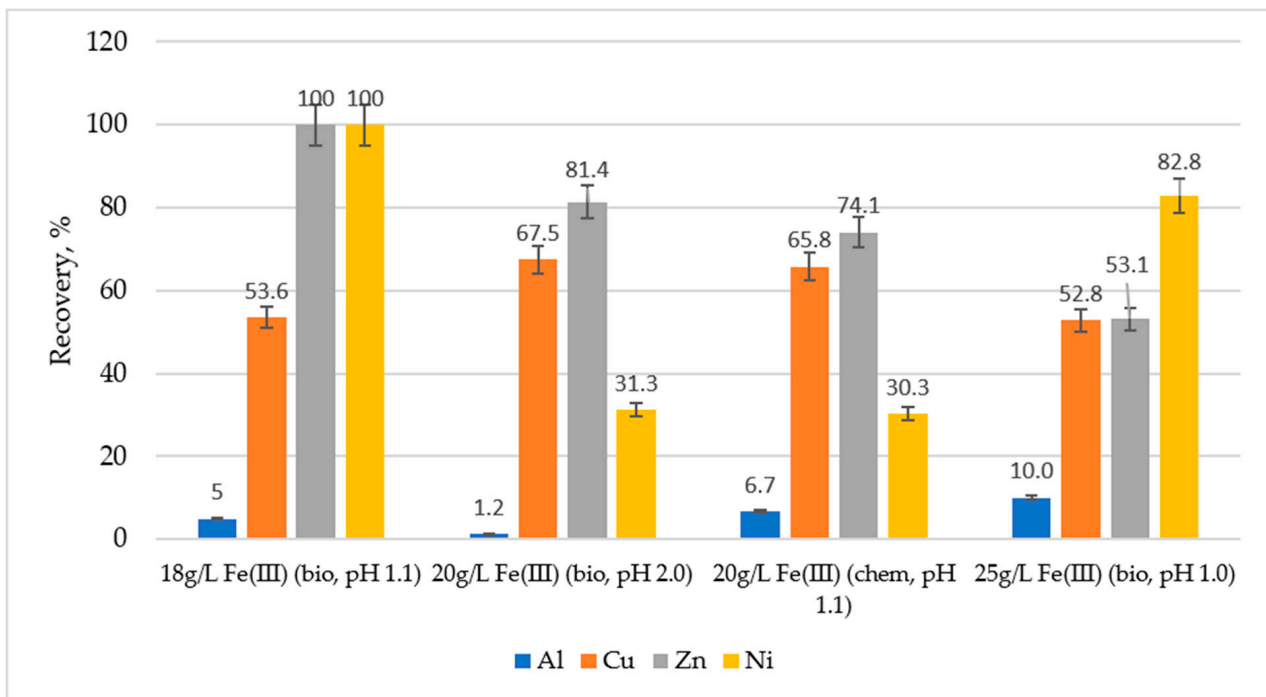


**Figure 5.** Metals recovery from PCBs at various concentrations of chemical and biogenic  $\text{Fe}^{3+}$  and pH (PD 5%; 40 °C, air 1 lpm; 600 rpm; duration 24 h).

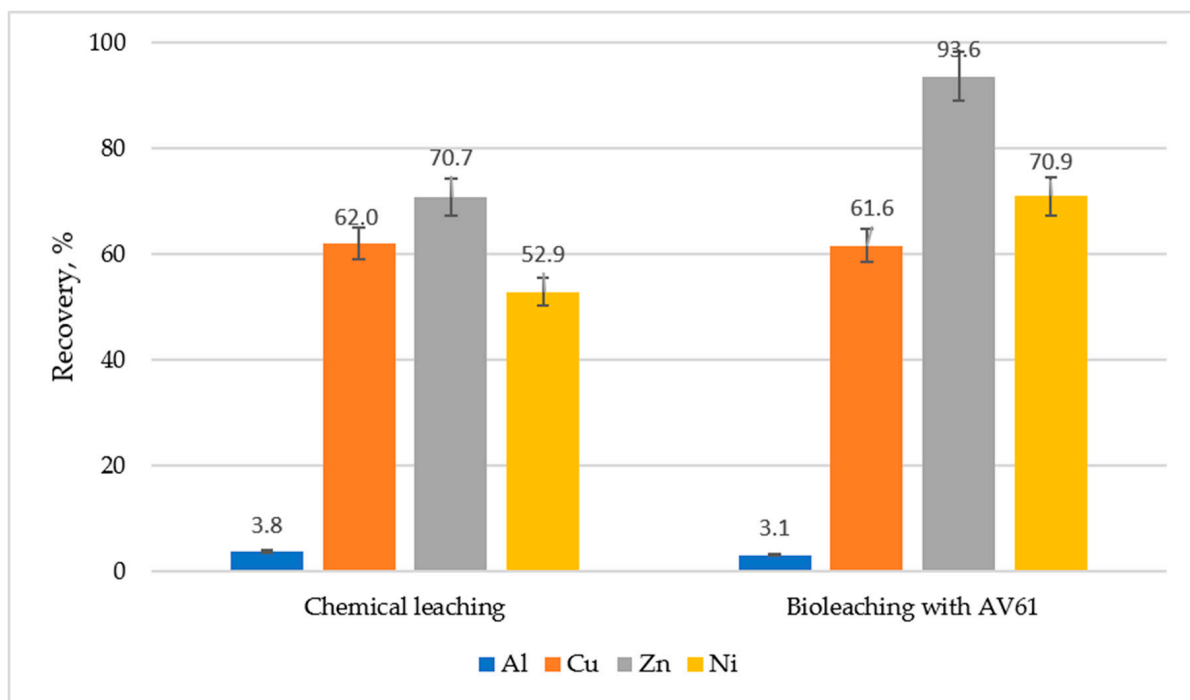


**Figure 6.** Recovery of metals from PCBs with two-stage leaching, 6 h duration (2 h + 4 h). (PD 10%;  $\text{Fe}^{3+}$  concentration 16 g/L (chem) and 19 g/L (bio); initial pH 1.2; 40 °C; air 1 lpm; 600 rpm.)

Cumulative metal content in the PLS during each of the two stages is plotted for each metal in Figure 7 to demonstrate the effect of ferric iron origin. It can be noted that Cu dissolution by biogenic  $\text{Fe}^{3+}$  occurred mostly during the first stage, while in case of chemical leaching, Cu dissolution rate was identical in both stages. The recovery of Zn was, on the other hand, more pronounced during the second stage in both leaching



systems. The majority of Ni occurred in solution over the first stage of the chemical-assisted leaching, while in the case of biogenic  $\text{Fe}^{3+}$ , Ni dissolution rate was identical in both stages. Aluminum was brought in solution in majority during the first step.

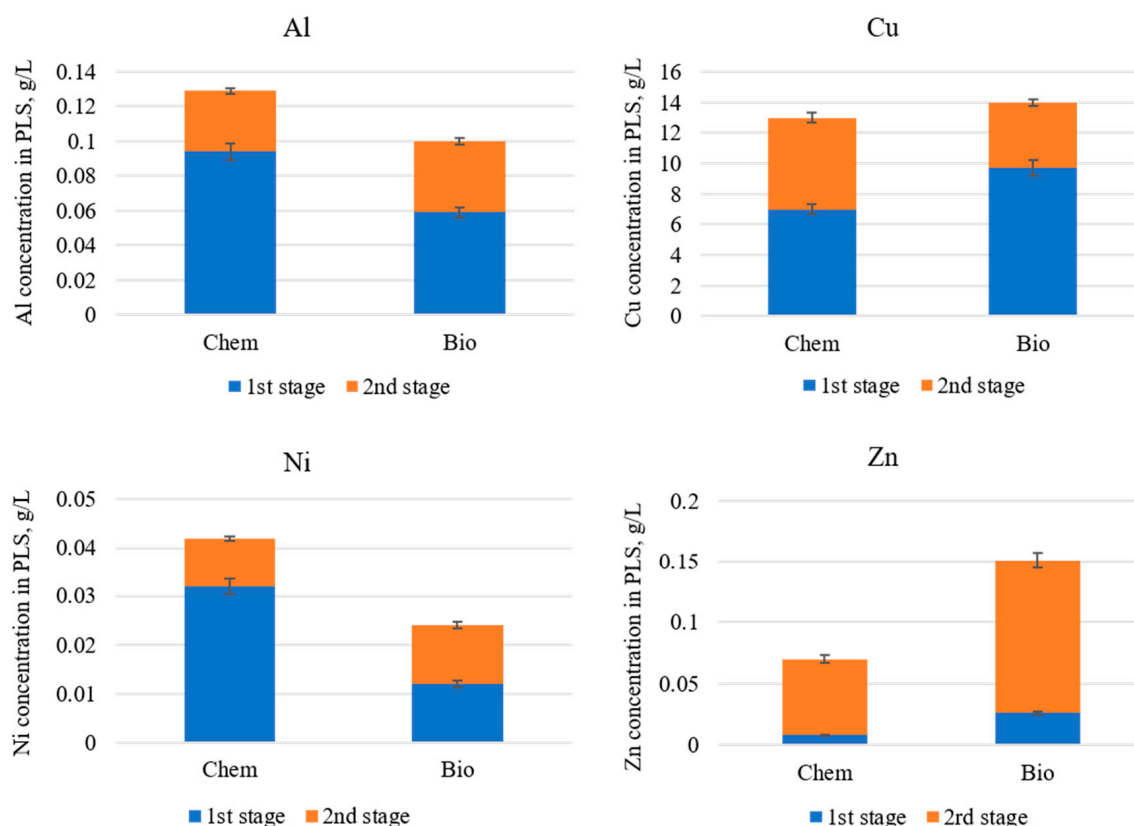


**Figure 7.** Cumulative metal content of the pregnant leach solution (PLS) after two-stage leaching with bio- and chemically generated  $\text{Fe}^{3+}$  (PD 10%; initial pH 1.2; 40 °C; air 1 lpm; 600 rpm).

Since the intrinsic value of the PCBs tested in the present study is to a larger extent due to Cu content, it was important to follow the kinetics of Cu bioleaching, and at the same time to perform iron speciation inside the process. Moreover, it was interesting to verify through cell enumeration if bacterial activity was maintained during leaching.

Figure 8 illustrates the copper content in PLS and iron speciation during the sampling performed at each hour of the two-stage process. During the first stage, copper seems to be brought in solution more easily thanks to the abundant availability of biogenic  $\text{Fe}^3$ . Ferric iron was almost consumed after two hours, dropping from 20 g/L to less than 3 g/L. During the second stage, the addition of fresh biolixiviant enabled us to bring out most of the remaining Cu in solution, however, not to a complete extent. Cu leaching almost halted after 4 h regardless of the ferric iron still being present. This was probably because part of the Cu in the PCBs existed in non-leachable form (alloy, oxidized, locked).

Note that after 24 h of leaching there was a distinct reduction in bacterial population in the PLS—from  $10^9$  to  $10^1$  cells/mL—as shown in Table 2. This phenomenon seemed intuitive due to the inhibitory effect of PCBs on bacterial activity given their heterogenous composition carrying variety of hazardous compounds.

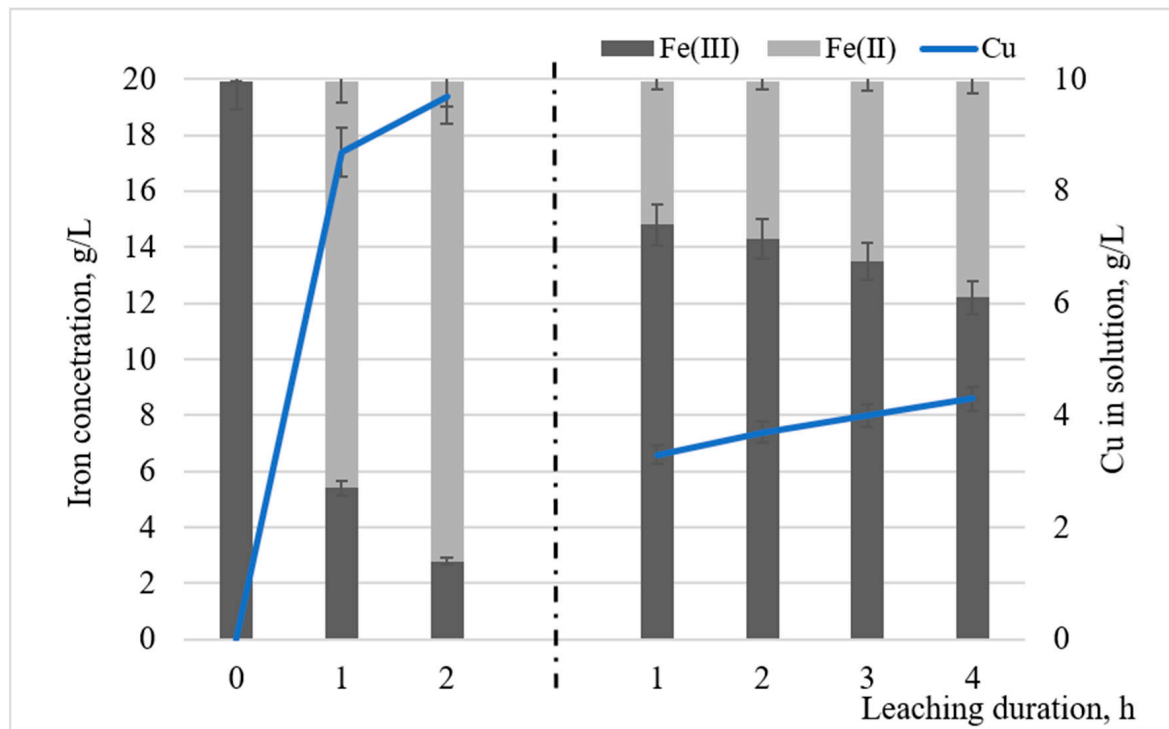


**Figure 8.** Kinetics of two-stage Cu leaching and iron speciation in the biogenic  $\text{Fe}^{3+}$  system.

**Table 2.** Bacteria enumeration during bioleaching (PD 5%, initial pH-2.0, 20 g/L  $\text{Fe}^{3+}$ , 40 °C, air -1 lpm, 600 rpm, duration-24 h).

Duration	Number of Cells, Cells/mL
Initial (0 min)	$0.6 \times 10^9$
1 h	$0.25 \times 10^7$
3 h	$0.6 \times 10^5$
5 h	$0.25 \times 10^5$
24 h	$0.6 \times 10$

The oxidation–reduction potential (ORP) is an important metric that reflects the oxidation and reduction reactions taking place in the medium. Before bioleaching, the ORP of the bacterial solution was as high as 671 mV and 606 mV (Ag/AgCl) at pH 1.1 and 2, respectively. After one hour of leaching, ORP dropped sharply to 423 mV and 428 mV (Ag/AgCl), respectively, due to the reduction of  $\text{Fe}^{3+}$  ions to  $\text{Fe}^{2+}$ —Figure 9. After the first hour and until the tests end, ORP declined at a slower pace from 423 and 428 to 400 and 354 mV (Ag/AgCl), respectively.

Analysis of Figure 9 also shows that the initial pH increased over the course of the bioleaching. This increase may have resulted from the alkaline compounds found in the PCBs, which were consumed due to the acidic action of the bacterial culture. Furthermore, the increase in pH may have resulted from the bacterial oxidation of  $\text{Fe}^{2+}$  to  $\text{Fe}^{3+}$  (see Equation (2)), which is known as an acid (proton) consumption process. As seen from Figure 9, the initial pH of 1.1 and 2 increased to 1.5 and 2.6, respectively, after 24 h, resulted in precipitation of  $\text{Fe}^{3+}$  in the form of jarosite. It might be that metallic particles trapped inside the jarosite were reflected in a lower overall leaching efficiency for all the metals.

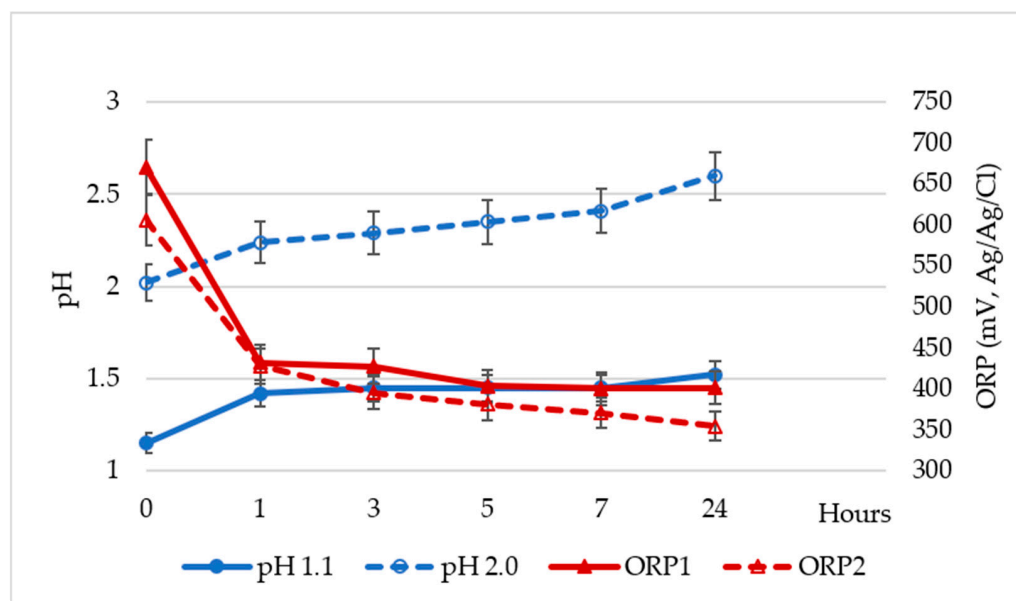


**Figure 9.** Variation of pH and ORP during bioleaching of PCBs (PD 5%; initial pH 2.0; 20 g/L  $\text{Fe}^{3+}$ ; 40 °C, air 1 lpm; 600 rpm; duration 24 h).

### 3.2. Mineralogy of the Leached PCBs

The reddish-brown precipitate observed after PCBs bioleaching was collected and sent for mineralogical analysis, being determined as jarosite—Figure 10.

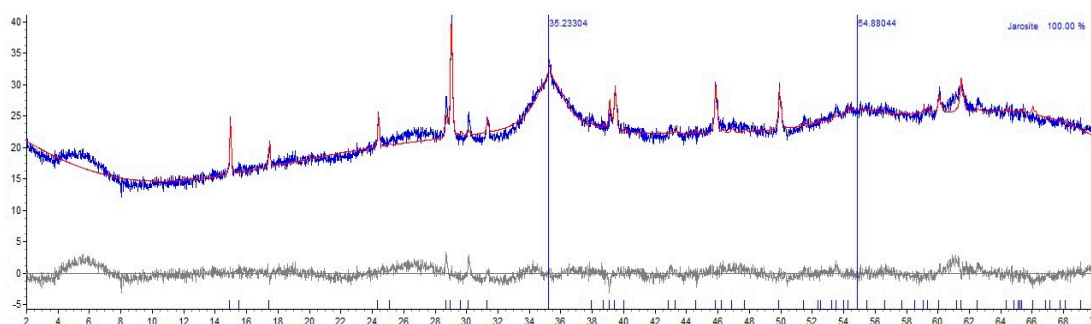


**Figure 10.** Mineralogy of a residue (jarosite) after bioleaching of PCBs (bio  $\text{Fe}^{3+}$  20 g/L; PD 5%; 40 °C; air 1 lpm; 600 rpm, pH 2).

From Figure 10 it can be seen that the occupancy factor for the K site was very high, which may indicate other heavy atoms on that site (Ag, Pb or Ba). The background was also high, indicating the presence of amorphous phases. As noted earlier in the Materials and Methods, given the PCBs' composition, in 100 g of PCB we could expect 3.2 g Pb, 1.98 g Sn and 0.097 g Ag. In view of the elevated content of Pb and the low amount of Ag in our samples, it was likely that the very large electronic density observed in the large site of jarosite was mainly due to Pb presence. This was supported by the known low dissolution degree of Pb in acidic media, which remained in the PCBs, a fact being in accordance with the literature [60]. It has to be noted that a higher amount of jarosite precipitation was observed when pH was kept around 2.

### 3.3. Visual Appearance of PCBs before and after Leaching

It was important to visually characterize and follow the chemical composition evolution of the remaining PCBs after the leaching through SEM-EDS inspection. Figures 11 and 12 illustrate images from a PCB sample before leaching. The backscattered electrons (BSE) images provided signals from a polished section in grayscale (Figures 11a and 12a)

making it possible to distinguish plastics (dark) from metallic particles (bright) thanks to their chemical composition contrast. As atomic numbers of the metal (e.g., Cu, Zn) carriers are close proximity range, the level of brightness could be similar, rendering their distinguishing difficult. Therefore, extra information acquired from energy dispersive spectroscopy (EDS) was considered, enabling us to differentiate the composition of the metallic particles—Figures 11b and 12b.

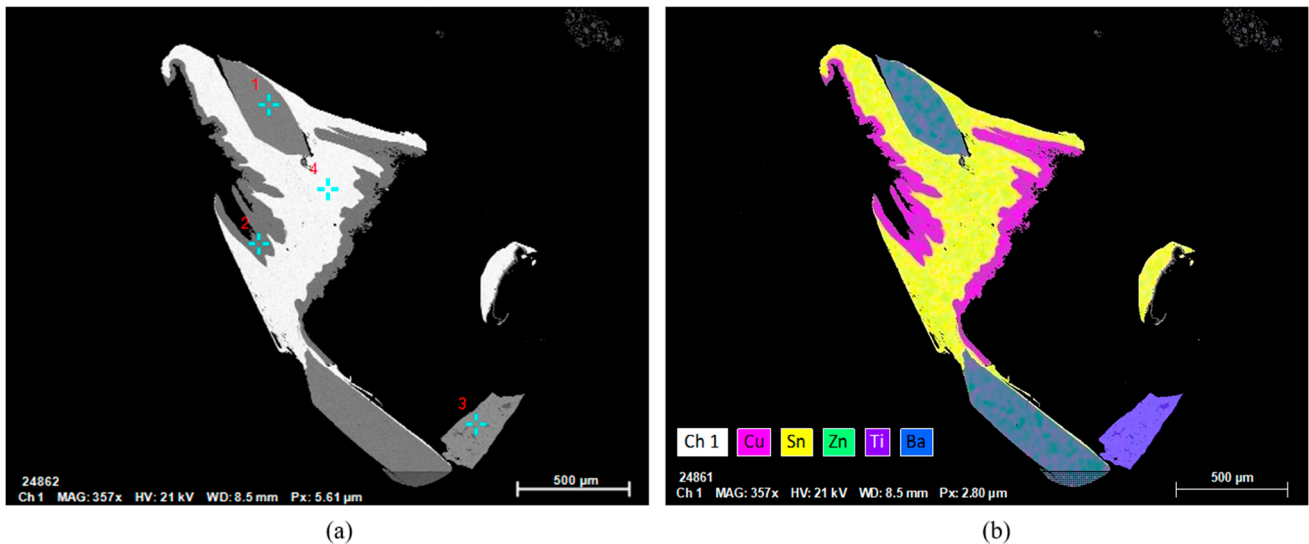


**Figure 11.** Micrograph (BSE-SEM) of a feed PCB, (a) BSE-SEM image; (b) EDS-SEM image.

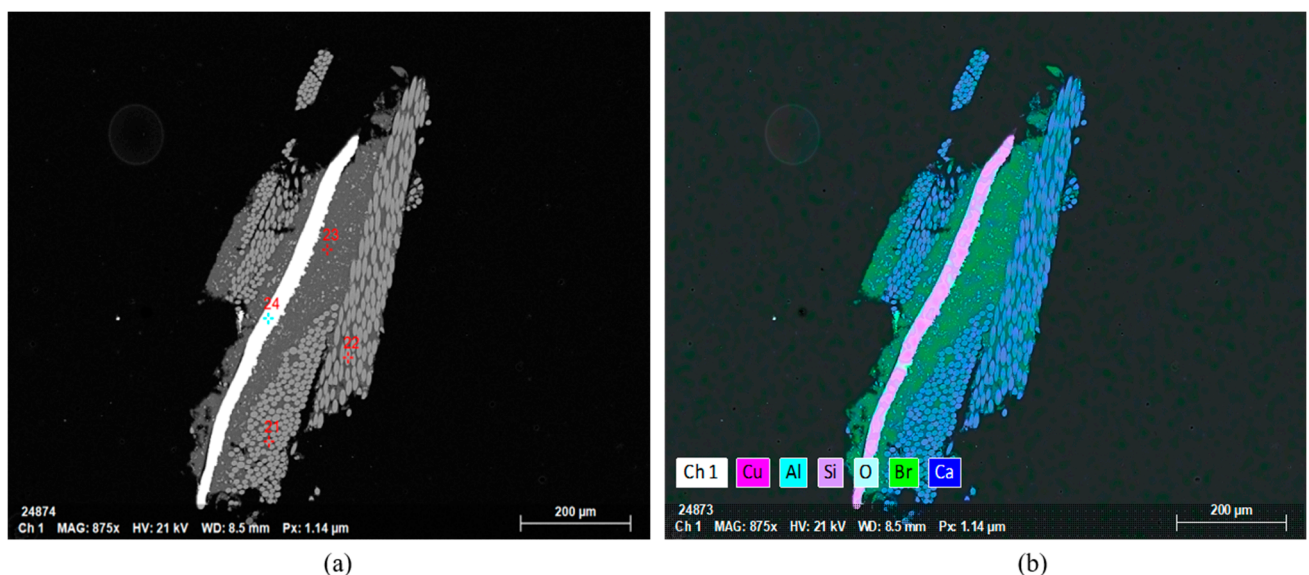


**Figure 12.** Micrographs (BSE-SEM) of a feed PCB, (a) BSE-SEM image; (b) EDS-SEM image.

Analysis of the images in Figure 11a shows flagged composite particles (probably fiberglass or silica laminate) and metals being partly interlocked inside the same PCB piece. Figure 11b shows that tin (Sn) belonging more likely to a soldering material was met in the fragmented PCBs as a single fragment and as joined with copper assemblage.

A situation similar to the one seen in Figure 11 was observed in Figure 12, with non-liberated Cu being wrapped within inert layers, possibly fiberglass.

After leaching completion, the leached residue was recovered as two different granulometric fractions: “coarse” (1–2 mm) and “fine” (below 1 mm). Figure 13 provides view of a “coarse” leached residue indicating presence of copper surrounded by a fiberglass layers.

Two relatively large particles of encapsulated native Cu were visible. The EDS chemistry of points 3–5 mapped in Figure 13 are shown in Table 3. The EDS mapping revealed that the two visible copper fragments were surrounded by Sn with traces of jarosite, and likewise silicon, the latter being part of the PCB composite matrix—EDS points 4 and 5.

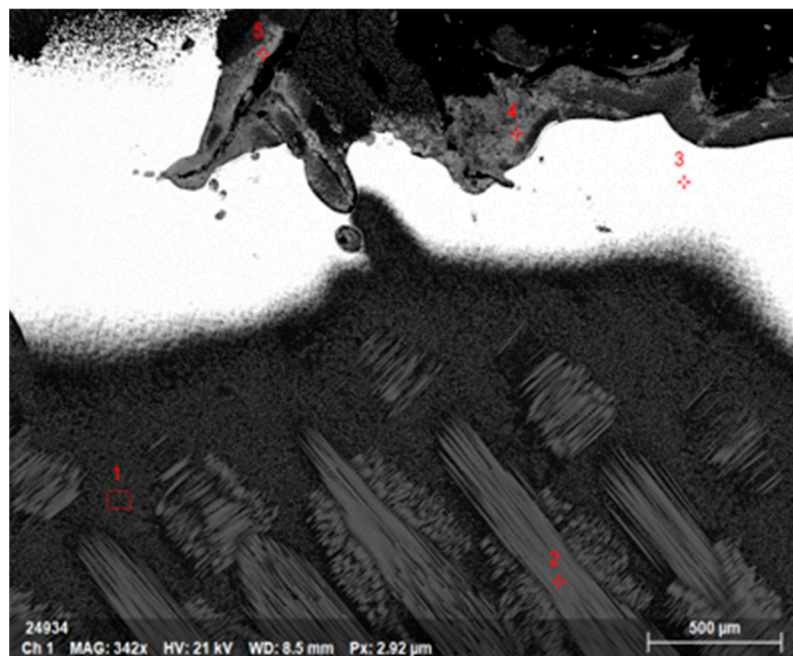


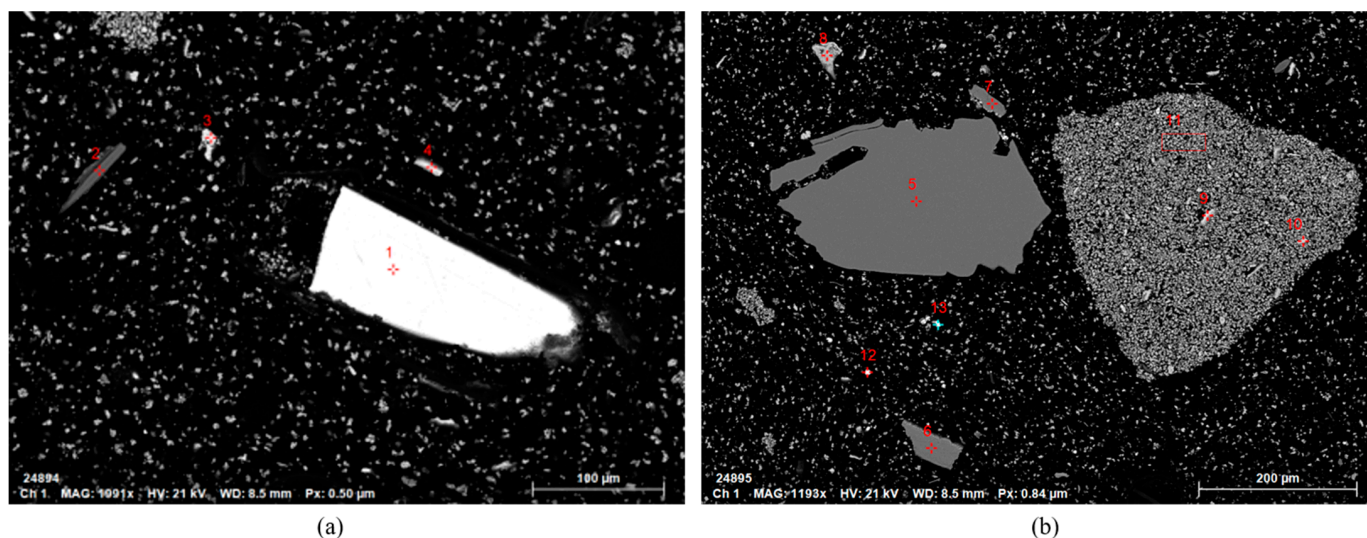
Figure 13. Micrograph (BSE-SEM) of a leached PCB (“coarse” fraction).

Table 3. EDS mapping of leached PCB (%) (“coarse” residue shown in Figure 13).

Spectrum	Oxygen	Aluminum	Silicon	Phosphorus	Sulfur	Calcium	Iron	Copper	Bromine	Tin
1	40.22		20.65			13.11		4.17	21.85	
2	45.45	8.76	21.5			17.39		1.45	5.45	
3								100		
4	36.09		1.84	4.76	0.87	1.25	10.74	2.69	17.3	24.46
5	29.21		0.95	5.91	1.36		17.42	4.01	4.3	36.85

The above observations could explain the impossibility to overcome 87% copper leaching even at a lower PD of 1%. It seems that the liberation degree resulting from the fragmentation of the PCBs was sufficient to release native copper to a certain degree; however, part of it remained trapped inside the PCBs layering.

Figure 14a illustrates a native copper fragment found in the fine residue, seen as spectrum 1 in Table 4, together with two finer Cu-Sn-bearing particles—spectra 3 and 4. This finding would indicate that passivation may have occurred during the leaching or that the hydrodynamic conditions were not optimal with possible creation of dead zones inside the reactor, allowing part of the material to escape from contact with the leachate. The rest of the finer fraction was composed of heterogenous, mixed with all different components present in the PCBs, which were not leachable—Figure 14b.



**Figure 14.** Micrographs (BSE-SEM) of a leached PCB (“fine” fraction), (a) and (b) BSE-SEM images of “fine” fraction.

**Table 4.** EDS mapping of leached PCB (%) (“fine” residue shown in Figure 14a).

Spectrum	Al	Si	P	S	Ca	Fe	Cu	Sn
1							100	
2	8.87	24.86			17.82		5.68	
3		0.57	3.03	0.78		13.07	6.51	53.33
4			2.46	1.2		15.22	8.12	50.13

#### 4. Conclusions

Several leaching experiments were performed on a fragmented end-of-life printed circuit board samples (21.2 wt% Cu, 1 wt% Zn, 0.1 wt% Ni, 2.2 wt% Al) pre-treated in NaOH solution to remove the protective organic coating, while the pulp density, initial pH,  $\text{Fe}^{3+}$  origin and number of leaching steps were varied.

It was determined that indirect bioleaching outperformed chemical leaching when realized under a two-stage mode. During bioleaching, the relative amount of  $\text{Fe}^{3+}$  decreased while a proportionate amount of jarosite was generated. The corresponding trend of pH was the opposite of the one for  $\text{Fe}^{3+}$ . For the highest degree of pulp density (10%), the copper leaching efficiency for both chemical and biological route was nearly similar—62%.

At the lowest pulp density (1%), 87% bioleaching of copper was achieved at 15.5 g/L initial  $\text{Fe}^{3+}$  concentration. There was an observed difference in the leaching efficiency of nickel as function of the initial concentration of  $\text{Fe}^{3+}$  and pH. Nearly 100% recovery was observed at 5% pulp density, 18 g/L  $\text{Fe}^{3+}$  and pH 1.1. As for zinc, the bio-assisted leaching system brought more improvement in leaching efficiency. A double-stage bioleaching with a total duration of 6 h and 10% pulp density led to 61% Cu recovery.

Microscopical inspection of input PCBs and leached residues confirmed that metals were not entirely liberated from their surrounding matrix, which reflected in incomplete leaching. The intrinsic form under which metals are present in the PCBs (alloys, oxides) also plays role in their leachability.

The approach presented in this study enabled us to outline the optimal bioleaching parameters to maximize or achieve the given recovery criteria for non-ferrous metals contained in the PCBs. The results open an avenue for further investigations with the ultimate aim of rendering bioleaching as an enabling technology for urban mining of metals from low-grade WEEE streams that usually escape from the mainstream metallurgical processing routes.

The limitation of the suggested method could be the concentration of  $\text{Fe}^{3+}$  (lixiviant). To solve this problem, we intent to carry out bioleaching in two stages using an additional amount of  $\text{Fe}^{3+}$  in the second stage. In order to obtain up-scalable results, tests in larger volume reactors (5 L) that allow for a larger amount of homogenized input material to be treated are underway.

**Author Contributions:** Conceptualization, A.V. and S.G.; methodology, A.V. and S.G.; validation, A.V., M.A., N.V., P.M. and S.G.; formal analysis, A.V.; investigation, A.V.; resources, N.V. and S.G.; data curation, A.V.; writing—original draft preparation, A.V.; writing—review and editing, M.A., P.M., N.V. and S.G.; visualization, S.G.; supervision, S.G.; funding acquisition, S.G. All authors have read and agreed to the published version of the manuscript.

**Funding:** This research has been funded by ERAMIN-2 Call 2019, BaCLEM project (Walloon region grant n 2010023).

**Data Availability Statement:** Not applicable.

**Acknowledgments:** A.K. Vardanyan is grateful to the Wallonia-Brussels International (WBI) Post-doctoral Excellence Grant and the Science Committee of the Republic of Armenia Research grant no 21T-1F124. The authors are thankful to F. Hattert and H. Bouzahzah for the XRD and SEM-EDS analysis and interpretations.

**Conflicts of Interest:** The authors declare no conflict of interest.

## References

1. Kumari, A.; Jha, M.; Singh, R.P. Recovery of metals from pyrolyzed PCBs by hydrometallurgical techniques. *Hydrometallurgy* **2016**, *165*, 97–105. [[CrossRef](#)]
2. Hadi, P.; Xu, M.; Lin, C.S.K.; Hui, C.-W.; McKay, G. Review: Waste printed circuit board recycling techniques and product utilization. *J. Hazard. Mater.* **2015**, *283*, 234–243. [[CrossRef](#)] [[PubMed](#)]
3. Sodha, A.B.; Shah, M.B.; Qureshi, S.A.; Tipre, D.R.; Dave, S.R. Decouple and compare the role of abiotic factors and developed iron and sulfur oxidizers for enhanced extraction of metals from television printed circuit boards. *Sep. Sci. Technol.* **2019**, *54*, 4. [[CrossRef](#)]
4. Sadia, I.; Srivastava, R.R.; Kima, H.; NimraI, I. Biotechnological recycling of hazardous waste PCBs using *Sulfobacillus thermosulfidooxidans* through pretreatment of toxicant metals: Process optimization and kinetic studies. *Chemosphere* **2022**, *286*, 131978.
5. Islam, A.; Ahmed, T.; Awual, M.R.; Rahman, A.; Sultana, M.; Aziz, A.A.; Monir, M.U.; Teo, S.H.; Hasan, M. Advances in sustainable approaches to recover metals from e-waste—A review. *J. Clean. Prod.* **2020**, *244*, 118815. [[CrossRef](#)]
6. Lehner, T. Integrated recycling of non-ferrous metal at Boliden Ltd. In Proceedings of the 1998 IEEE International Symposium on Electronics and the Environment, Oak Brook, IL, USA, 6 May 1998; pp. 42–47.
7. Bleiwas, D.; Kelly, T. *Obsolete Computers, “Gold Mines”, or High-Tech Trash? Resource Recovery from Recycling*; United States Geological Survey 7; USDS: Beaverton, OR, USA, 2001. [[CrossRef](#)]
8. He, W.; Li, G.; Ma, X.; Wang, H.; Huang, J.; Xu, M.; Huang, C. WEEE recovery strategies and the WEEE treatment status in China. *J. Hazard. Mater.* **2006**, *136*, 502–512. [[CrossRef](#)]
9. Deveci, H.; Yazıcı, E.Y.; Aydın, U.; Yazıcı, R.; Akcil, A. Extraction of copper from scrap TV boards by sulphuric acid leaching under oxidising conditions. In Proceedings of the Going Green-CARE INNOVATION 2010 Conference (2010), Vienna, Austria, 8–11 November 2010; p. 45.
10. Kaya, M. Recovery of metals from electronic waste by physical and chemical recycling processes. *Int. J. Chem. Mol. Nucl. Mater. Metall. Eng.* **2016**, *10*, 232–243. [[CrossRef](#)]
11. Moyo, T.; Chirume, B.H.; Petersen, J. Assessing alternative pre-treatment methods to promote metal recovery in the leaching of printed circuit boards. *Resour. Conserv. Recycl.* **2020**, *152*, 104545. [[CrossRef](#)]
12. Dave, S.; Sodha, A.; Tipre, D. Microbial technology for metal recovery from e-waste printed circuit boards. *J. Bacteriol. Mycol.* **2018**, *6*, 241–247. [[CrossRef](#)]
13. Vasile, C.; Brebu, M.A.; Totolin, M.; Yanik, J.A.L.E.; Karayildirim, T.A.M.E.R.; Darie, H. Feedstock recycling from the printed circuit boards of used computers. *Energy Fuels* **2008**, *22*, 1658–1665. [[CrossRef](#)]
14. Birloaga, I.; De Michelis, I.; Ferella, F.; Buzatu, M.; Vegliò, F. Study on the influence of various factors in the hydrometallurgical processing of waste printed circuit boards for copper and gold recovery. *Waste Manag.* **2013**, *33*, 935–941. [[CrossRef](#)] [[PubMed](#)]
15. Oishi, T.; Koyama, K.; Alam, S.; Tanaka, M.; Lee, J.C. Recovery of high purity copper cathode from printed circuit boards using ammoniacal sulfate or chloride solutions. *Hydrometallurgy* **2007**, *89*, 82–88. [[CrossRef](#)]
16. Fogarasi, S.; Imre-Lucaci, F.; Imre-Lucaci, Á.; Ilea, P. Copper recovery and gold enrichment from waste printed circuit boards by mediated electrochemical oxidation. *J. Hazard. Mater.* **2014**, *273*, 215–221. [[CrossRef](#)] [[PubMed](#)]

17. Hubau, A.; Minter, M.; Changes, A.; Jouliau, C.; Silvente, C.; Guezennec, A.G. Recovery of metals in a double-stage continuous bioreactor for acid bioleaching of printed circuit boards (PCBs). *Sep. Purif. Technol.* **2020**, *238*, 116481. [[CrossRef](#)]
18. Sodha, A.; Qureshi, S.; Khatri, B.; Tipre, D.; Dave, S. Enhancement in iron oxidation and multi-metal extraction from waste television printed circuit boards by iron oxidizing *Leptospirillum feriphillum* isolated from coal sample. *Waste Biomass Valor.* **2017**, *10*, 671–680. [[CrossRef](#)]
19. Jadhav, U.; Hocheng, H. Enzymatic bioleaching of metals from printed circuit board. *Clean Technol. Environ. Policy* **2015**, *17*, 947–956. [[CrossRef](#)]
20. Kiddee, P.; Naidu, R.; Wong, M.H. Metals and polybrominated diphenyl ethers leaching from electronic waste in simulated landfills. *J. Hazard. Mater.* **2013**, *252–253*, 243–249. [[CrossRef](#)]
21. Mankhand, T.; Singh, K.; Kumar, S.; Gupta, S.; Das, S. Pyrolysis of printed circuit boards. *Int. J. Metall. Mater. Sci. Eng.* **2012**, *6*, 102–107. [[CrossRef](#)]
22. Akcil, A.; Erust, C.; Sekhar, G.C.; Ozgun, M.; Sahin, M.; Tuncuk, A. Precious metal recovery from waste printed circuit boards using cyanide and non cyanide lixivants—A review. *Waste Manag.* **2015**, *45*, 258–271. [[CrossRef](#)] [[PubMed](#)]
23. Jadhao, P.; Chauhan, G.; Pant, K.K.; Nigam, K.D.P. Greener approach for the extraction of copper metal from electronic waste. *Waste Manag.* **2015**, *57*, 102–112. [[CrossRef](#)]
24. Krebs, W.; Brombacher, C.; Bosshard, P.P.; Bachofen, R.; Brandl, H. Microbial recovery of metals from solids. *FEMS Microbiol. Rev.* **1997**, *20*, 605–617. [[CrossRef](#)]
25. Vermeulen, F.; Nicolay, X. Sequential bioleaching of copper from brake pads residues using encapsulated bacteria. *Miner. Eng.* **2017**, *106*, 39–45. [[CrossRef](#)]
26. Tunchuk, A.; Stazi, V.; Akcil, A.; Yazici, E.Y.; Deveci, H. Aqueous metal recovery techniques from e-scrap: Hydrometallurgy in recycling. *Miner. Eng.* **2012**, *25*, 28–37. [[CrossRef](#)]
27. Mrazikova, A.; Kadukova, J.; Marcincakova, R.; Velgosova, O.; Willner, J.; Fornalczyk, A.; Saturnus, M. The effect of specific conditions on Cu, Ni, Zn and Al recovery from PCBs waste using acidophilic bacterial strains. *Arch. Metall. Mater.* **2016**, *61*, 261–264. [[CrossRef](#)]
28. Tapia, J.; Duenas, A.; Cheje, N.; Socle, G.; Patino, N.; Ancalla, W.; Tenorio, S.; Denos, J.; Taco, H.; Cao, W.; et al. Bioleaching of heavy metals from printed circuit boards with an Acidophilic iron-oxidizing microbial consortium in stirred tank reactor. *Bioengineering* **2022**, *9*, 79. [[CrossRef](#)] [[PubMed](#)]
29. Modin, O.; Fuad, N.; Rauch, S. Microbial electrochemical recovery of zinc. *Electrochim. Acta.* **2017**, *248*, 58–63. [[CrossRef](#)]
30. Hong, Y.; Valix, M. Bioleaching of electronic waste using acidophilic sulfur oxidizing bacteria. *J. Clean. Prod.* **2014**, *65*, 465–472. [[CrossRef](#)]
31. Brandl, H.; Bosshard, R.; Wegmann, M. Computer-munching microbes: Metal leaching from electronic scrap by bacteria and fungi. *Hydrometallurgy* **2001**, *59*, 319–326. [[CrossRef](#)]
32. Yang, C.; Zhu, N.; Shen, W.; Zhang, T.; Wu, P. Bioleaching of copper from metal concentrates of waste printed circuit boards by a newly isolated *Acidithiobacillus ferrooxidans* strain Z1. *J. Mater. Cycles Waste Manag.* **2017**, *19*, 247–255. [[CrossRef](#)]
33. Zhu, N.; Xiang, Y.; Zhang, T.; Wu, P.; Danga, Z.; Li, P.; Wu, J. Bioleaching of metal concentrates of waste printed circuit boards by mixed culture of acidophilic bacteria. *J. Hazard. Mater.* **2011**, *192*, 614–619. [[CrossRef](#)] [[PubMed](#)]
34. Xia, M.C.; Wang, Y.P.; Peng, T.J.; Shen, L.; Yu, R.L.; Liu, Y.D.; Chen, M.; Li, J.K.; Wu, X.L.; Zeng, W.M. Recycling of metals from pretreated waste printed circuit boards effectively. *J. Biosci. Bioeng.* **2017**, *123*, 714–721. [[CrossRef](#)] [[PubMed](#)]
35. Mahmoud, A.; Cezac, P.; Hoadley, A.F.; Contamine, F.; D’hugues, P. A review of sulfide minerals microbially assisted leaching in stirred tank reactors. *Int. Biodeterior. Biodegrad.* **2017**, *119*, 118–146.
36. Murrugesan, M.P.; Kannan, K.; Selvaganapathy, T. Bioleaching recovery of copper from printed circuit boards and optimization of various parameters using response surface methodology (RSM). *Mater. Today Proc.* **2020**, *26 Pt 2*, 2720–2728. [[CrossRef](#)]
37. Ilyas, S.; Anwar, M.A.; Niazi, S.; Ghauri, M.A. Bioleaching of metals from electronic scrap by moderately thermophilic acidophilic bacteria. *Hydrometallurgy* **2007**, *88*, 180–188. [[CrossRef](#)]
38. Shah, M.; Tipre, D.; Purohit, M.; Dave, S. Development of two-step process for enhanced biorecovery of Cu-Zn-Ni from computer printed circuit boards. *J. Biosci. Bioeng.* **2015**, *120*, 167–173. [[CrossRef](#)]
39. Marques, A.C.; Cabrera, J.M.; Malfatti, C.F. Printed circuit boards: A review on the perspective of sustainability. *J. Environ. Manag.* **2013**, *131*, 298–306. [[CrossRef](#)] [[PubMed](#)]
40. Liang, G.; Tang, J.; Liu, W.; Zhou, Q. Optimizing mixed culture of two acidophiles to improve copper recovery from printed circuit boards (PCBs). *J. Hazard. Mater.* **2013**, *250–251*, 238–245. [[CrossRef](#)] [[PubMed](#)]
41. Jagannath, A.A.; Shetty, V.K.; Saidutta, M.B. Bioleaching of copper from electronic waste using *Acinetobacter* sp. Cr B2 in a pulsed plate column operated in batch and sequential batch mode. *J. Environ. Chem. Eng.* **2017**, *5*, 1599–1607. [[CrossRef](#)]
42. Anshu, P.; Subrata, H. Feasibility of bioleaching of selected metals from electronic waste by *Acidiphilium acidophilum*. *Waste Biomass Valorization* **2017**, *9*, 871–877. [[CrossRef](#)]
43. Amiri, F.; Mousavi, S.M.; Yaghmaei, S.; Barati, M. Bioleaching kinetics of a spent refinery catalyst using *Aspergillus niger* at optimal conditions. *Biochem. Eng. J.* **2012**, *67*, 208–217. [[CrossRef](#)]
44. Santhiya, D.; Ting, Y.P. Use of adapted *Aspergillus niger* in the bioleaching of spent refinery processing catalyst. *J. Biotechnol.* **2006**, *121*, 62–74. [[CrossRef](#)] [[PubMed](#)]



45. Falguni, P.; Lakshmi, B. Bioleaching of copper and nickel from mobile phone printed circuit board using *Aspergillus fumigatus* A2DS. *Environ. Chem. Lett.* **2019**, *17*, 1873–1879.
46. Pradhan, J.; Kumar, S. Metals bioleaching from electronic waste by *Chromobacterium violaceum* and *Pseudomonads* sp. *Waste Manag. Res.* **2012**, *30*, 1151–1159. [[CrossRef](#)] [[PubMed](#)]
47. Tay, S.B.; Natarajan, G.; Abdul Rahim, M.N.; Tan, H.T.; Chung, M.C.; Ting, Y.P.; Yew, W.S. Enhancing gold recovery from electronic waste via lixiviant metabolic engineering in *Chromobacterium violaceum*. *Sci. Rep.* **2016**, *3*, 2236. [[CrossRef](#)] [[PubMed](#)]
48. Shin, D.; Jeong, J.; Lee, S.; Pandey, B.; Lee, J. Evaluation of bioleaching factors on gold recovery from ore by cyanide-producing bacteria. *Miner. Eng.* **2013**, *48*, 20–24. [[CrossRef](#)]
49. Hubau, A.; Minter, M.; Changes, A.; Jouliau, C.; Perez, C.; Guezennec, A.G. Continuous production of a biogenic ferric iron lixiviant for the bioleaching of printed circuit boards (PCBs). *Hydrometallurgy* **2018**, *180*, 180–191. [[CrossRef](#)]
50. Bas, A.D.; Deveci, H.; Yazici, E.Y. Bioleaching of copper from low grade scrap TV circuit boards using mesophilic bacteria. *Hydrometallurgy* **2013**, *138*, 65–70. [[CrossRef](#)]
51. Guezennec, A.G.; Jouliau, C.; Delort, C.; Bodenau, F.; Hedrich, S.; d’Hugues, P. CO<sub>2</sub> mass transfer in bioleaching reactors: CO<sub>2</sub> enrichment applied to a complex copper concentrate. *Hydrometallurgy* **2018**, *180*, 277–286. [[CrossRef](#)]
52. Ilyas, S.; Ruan, C.; Bhatti, H.N.; Ghauri, M.A.; Anwar, M.A. Column bioleaching of metals from electronic scrap. *Hydrometallurgy* **2010**, *101*, 135–140. [[CrossRef](#)]
53. Sodha, A.B.; Tipre, D.R.; Dave, S.R. Optimisation of biohydrometallurgical batch reactor process for copper extraction and recovery from non-pulverized waste printed circuit boards. *Hydrometallurgy* **2020**, *191*, 105170. [[CrossRef](#)]
54. Boxall, N.J.; Cheng, K.Y.; Bruckard, W.; Kaksonen, A.H. Application of indirect non-contact bioleaching for extracting metals from waste lithium-ion batteries. *J. Hazard. Mater.* **2018**, *360*, 504–511. [[CrossRef](#)]
55. Yken, J.V.; Cheng, K.Y.; Boxall, N.J.; Nikoloski, A.N.; Moheimani, N.; Valix, M.; Sahajwalla, V.; Kaksonen, A.H. Potential of metals leaching from printed circuit boards with biological and chemical lixiviants. *Hydrometallurgy* **2020**, *196*, 105433. [[CrossRef](#)]
56. Erkmen, O. Practice 4—Most probable number technique. In *Microbiological Analysis of Foods and Food Processing Environments*; Elsevier: Amsterdam, The Netherlands, 2022; pp. 31–37.
57. Lucchesi, C.A.; Hirn, C.F. EDTA Titration of total Iron in Iron(II) and Iron(III) mixtures. Application to Iron driers. *Anal. Chem.* **1960**, *32*, 1191–1193. [[CrossRef](#)]
58. Bouzahzah, H.; Benzaazoua, M.; Mermillod-Blondin, R.; Pirard, E. A novel procedure for polished section preparation for automated mineralogy avoiding internal particle settlement. In Proceedings of the 12th International Congress for Applied Mineralogy (ICAM), Istanbul, Turkey, 10–12 August 2015.
59. Vardanyan, A.; Vardanyan, N.; Abrahamyan, N.; Aatach, M.; Gaydardzhiev, S. Sequential biologically assisted extraction of Cu and Zn from printed circuit boards (PCB). *Int. J. Environ. Stud.* **2022**. [[CrossRef](#)]
60. Guezennec, A.G.; Bru, K.; Jacob, J.; d’Hugues, P. Co-processing of sulfidic mining wastes and metal-rich post-consumer wastes by biohydrometallurgy. *Miner. Eng.* **2015**, *75*, 45–53. [[CrossRef](#)]